

1-21-2015

Uptake and accumulation of bulk and nanosized cerium oxide particles and ionic cerium by radish (*Raphanus sativus* L.).

Weilan Zhang

Southern Illinois University Carbondale

Stephen D. Ebbs

Southern Illinois University Carbondale, sebbs@plant.siu.edu

Craig Musante

The Connecticut Agricultural Experiment Station

Jason C. White

The Connecticut Agricultural Experiment Station

Cunmei Gao

Shanghai Ocean University

Follow this and additional works at: http://opensiuc.lib.siu.edu/pb_pubs

This document is the Accepted Manuscript version of a Published Work that appeared in final form in the *Journal of agricultural and food chemistry*, copyright © American Chemical Society after peer review and technical editing by the publisher. To access the final edited and published work see <http://dx.doi.org/10.1021/jf5052442>.

Recommended Citation

Zhang, Weilan, Ebbs, Stephen D., Musante, Craig, White, Jason C., Gao, Cunmei and Ma, Xingmao. "Uptake and accumulation of bulk and nanosized cerium oxide particles and ionic cerium by radish (*Raphanus sativus* L.)." *Journal of agricultural and food chemistry* 63, No. 2 (Jan 2015). doi:10.1021/jf5052442.

Authors

Weilan Zhang, Stephen D. Ebbs, Craig Musante, Jason C. White, Cunmei Gao, and Xingmao Ma

**Uptake and Accumulation of Bulk and Nano-sized Cerium Oxide Particles and
Ionic Cerium by Radish (*Raphanus sativus* L.)**

Weilan Zhang¹, Stephen D. Ebbs², Craig Musante³, Jason C. White³, Cunmei Gao^{1,4},
Xingmao Ma^{1,*}

¹Department of Civil and Environmental Engineering, Southern Illinois University;
Carbondale, IL, 62901

²Department of Plant Biology and Center for Ecology, Southern Illinois University,
Carbondale, IL, 62901

³Department of Analytical Chemistry, The Connecticut Agricultural Experiment Station,
123 Huntington Street, New Haven, CT 06504, USA

⁴College of Marine Sciences, Shanghai Ocean University, Shanghai, 201306, China

*Corresponding author

Xingmao Ma

Department of Civil and Environmental Engineering

Southern Illinois University Carbondale

Carbondale, IL, USA, 62901

Ph: 618-453-7774

Fax: 618-453-3044

Email: ma@engr.siu.edu

Abstract

The potential toxicity and accumulation of engineered nanomaterials (ENMs) in agricultural crops has become an area of great concern and intense investigation. Interestingly, while below ground vegetables are most likely to accumulate the highest concentrations of ENMs, little work has been done investigating the potential uptake and accumulation of ENMs for this plant group. The overall objective of this study was to evaluate how different forms of cerium (bulk cerium oxide, cerium oxide nanoparticles, and the cerium ion) affected the growth of radish (*Raphanus sativus L.*) and accumulation of cerium in the radish tissues. Ionic cerium (Ce^{3+}) had a negative effect on radish growth at 10 mg $CeCl_3$ /L while bulk cerium oxide (CeO_2) enhanced plant biomass at the same concentration. Treatment with 10 mg/L cerium oxide nanoparticles (CeO_2 NPs) had no significant effect on radish growth. Exposure to all forms of cerium resulted in the accumulation of this element in radish tissues, including the edible storage root. However, the accumulation patterns and their effect on plant growth and physiological processes varied with the characteristics of cerium. This study provides a critical frame of reference on the effects of CeO_2 NPs vs. their bulk and ionic counterparts on radish growth.

Keywords

Cerium oxide, Nanomaterials, Nanoparticles, Radish, Phytotoxicity, Plant uptake

1 **Introduction**

2

3 Nanotechnology is a rapidly expanding global industry. Engineered nanomaterials
4 (ENMs) with their size smaller than 100 nm in at least two dimensions are increasingly
5 found in commercial products. Due to their small size and large specific surface area,
6 ENMs exhibit novel and different physical, chemical and biological properties from their
7 bulk or ionic counterparts. These unique properties provide new opportunities to fight
8 diseases, enhance energy efficiency and improve the environment (1,2,3).

9 While the synthesis of ENMs adds desirable physical and/or chemical properties
10 over the bulk or ionic forms, the potential environmental health and safety implications of
11 ENM uses have become a serious concern. Previous research has shown that some ENMs
12 used in consumer products are released into the environment and many of these materials
13 are detected in wastewater streams (4,5,6). As one of the most commonly employed
14 nanomaterials, cerium oxide nanoparticles (CeO₂ NPs) have attracted great attention. The
15 potential toxicity of CeO₂ NPs (6-40 nm, unmodified) to bacteria, fish, and mammalian
16 cells has been reported (7,8). Plants play a critical role in maintaining ecosystem health
17 and function and as a food source for humans. Plant uptake of ENMs represents an
18 important pathway for human exposure to these nanoparticles through food consumption
19 (9). Consequently, investigation of the uptake and accumulation of ENMs by agricultural
20 crops is not only warranted but also critical to food safety and human health. However,
21 there are only a small number of studies in the literature that have addressed the
22 interactions of CeO₂ NPs with terrestrial plants (10-16). In one study, Wang et al. (10)
23 found that uncoated CeO₂ NPs (< 25nm) at 0.1-10 mg/L had a slightly positive effect on
24 tomato (*Solanum lycopersicum* L.) growth and yield (e.g. increased production of tomato

25 fruit at 10 mg/L). However, cerium was reportedly transported from roots to shoots and
26 accumulated in edible tissues, although the chemical form of Ce was not determined.
27 These authors further investigated the trans-generational effect of CeO₂ NPs and found
28 that second generation seedlings grown with seeds from treated parental plants with 10
29 mg/L CeO₂ NPs were significantly smaller and accumulated more cerium as compared to
30 seedlings generated from control plants (11). Ma et al. (12) studied how rare earth oxide
31 NPs affected root elongation and found that bare CeO₂ NPs with an average diameter of
32 7.2 ± 0.7 nm had no effects on rape (*Brassica napus* L.), radish (*Raphanus sativus* L.),
33 wheat (*Triticum aestivum* L.), cabbage (*Brassica oleracea* L.), tomato (*Lycopersicon*
34 *esculentum* L.), and cucumber (*Cucumis sativus* L.) at 2,000 mg/L. Rico et al. (13)
35 demonstrated that exposing rice seedlings to bare CeO₂ NPs with an average size of 231
36 ± 16 nm up to 500 mg/L for ten days caused no visible signs of toxicity. However, CeO₂
37 NPs induced a concentration-dependent modification of the oxidative stress and
38 antioxidant defense system in the rice seedlings. Several studies have reported the uptake
39 and accumulation of CeO₂ NPs by agricultural crops. For instance, Zhang and colleagues
40 (14) showed that 7 nm and 25 nm bare CeO₂ NPs were detected in cucumber tissues but
41 the transport of cerium from roots to shoots was limited. Zhao et al. (15) investigated the
42 effects of bare and alginate coated CeO₂ NPs on corn plants and reported that surface
43 coating and soil organic matter could promote the translocation of cerium in higher plants.
44 A recent study demonstrated that intact CeO₂ NPs (7 nm) were taken up by soybean roots
45 (16). In summary, CeO₂ NPs can be taken up by plants and accumulated in plant tissues,
46 but the majority of the NPs appeared to remain in the root tissues, raising concerns on the
47 heightened accumulation of ENMs by root vegetables.

48 Interestingly, even though the edible tissues of belowground vegetables often
49 have direct contact with soil-borne ENMs and present the highest potential for ENMs
50 accumulation in food crops, little attention has been paid to this important group of food
51 plants. In this study, radish (*Raphanus sativus* L.) was adopted as a model plant in that it
52 is a popular vegetable with high global consumption. In addition, radishes mature rapidly
53 in full sun and light, and can be harvested in 3-4 weeks, making it an ideal plant to study
54 the fate and impact of environmental chemicals on the development of belowground
55 vegetables. The objectives of this study were two-fold: 1) how does cerium in different
56 chemical forms (e.g. ionic cerium vs. cerium particles) and physical sizes affect the
57 growth of radish? (2) How extensively and differently will the radish tissues take up and
58 accumulate cerium in different forms and sizes? With these two objectives, we aimed to
59 fill some of the current knowledge gap on the possible differential accumulation of
60 cerium with different forms and particles sizes by plants. Even though detailed studies on
61 the cerium effect of essential physiological and biochemical processes are not the
62 concentration of this study, their interactions are important for mechanistic understanding
63 of the interactions of plants and nanoparticles and warrant further investigations.

64

65 **Materials and Methods**

66

67 **Chemicals**

68 Dispersions of CeO₂ NPs (10 wt. % in H₂O) and cerium chloride powder were
69 purchased from Sigma-Aldrich (St. Louis, MO). The bulk powder of CeO₂ was obtained
70 from Strem Chemicals, Inc. (Newburyport, MA). Hoagland solution (one-quarter
71 strength) was prepared by dissolving an appropriate amount of the modified Hoagland
72 basal salt mixture (Phytotechnology Laboratories, Lenexa, KS) with deionized water. The

73 size and morphology of CeO₂ NPs and the bulk suspensions were characterized by
74 transmission electron microscopy (TEM). The hydrodynamic size and zeta potential of
75 CeO₂ NPs in quarter strength Hoagland solution were measured with a dynamic light
76 scattering instrument (Malvern Zetasizer Nano-ZS90, NY).

77 **Seed germination and growth conditions**

78 The radish seeds [Cherriette (F1)] were obtained from Johnny's Selected Seeds
79 (Winslow, ME). Seeds were surface sterilized with 1.25% sodium hypochlorite solution
80 for 10 minutes and then rinsed with deionized water three times. The sterilized seeds
81 were germinated on moist filter paper in a Petri dish for 7 days. Healthy young seedlings
82 with similar size (7.5 -8 cm in height from the root tip to the tip of cotyledons) and stage
83 of development were transferred to 50 mL polypropylene centrifuge tubes containing
84 quarter strength Hoagland solution and were incubated in a growth cart with a 16 hrs-
85 light/8 hrs-dark cycle (28 °C) to allow the seedlings to further develop. The growth cart
86 was equipped with four T5 fluorescent tubes, providing a light intensity of approximately
87 104 $\mu\text{mol m}^{-2}\cdot\text{s}^{-1}$ of visible light (400 ~ 700 nm) at the height of plant leaves. After 7
88 days, the seedlings were transferred from the centrifuge tubes to 100 mL glass jars
89 containing 10 mg/L of bulk or nano-sized cerium oxide (CeO₂) or cerium chloride
90 (CeCl₃). Each jar had a floating lid made by Hareline 2 mm thin fly foam (Fishwest,
91 Sandy, UT) so that the plant roots were constantly submerged in the treatment solutions.
92 Due to the scarcity of information on the potential adsorption of cerium on foam surface,
93 it was assumed that the potential impact of foam on cerium bioavailability was
94 insignificant in this study. Four treatments were prepared, all in quarter strength
95 Hoagland solution: (1) control (no cerium treatment), (2) 10 mg/L CeO₂ NPs, (3) 10

96 mg/L CeO₂ bulk, and (4) 10 mg/L CeCl₃. The concentration of 10 mg/L was chosen
97 because this value is considered environmentally relevant (18) and our previous studies
98 also showed that CeO₂ NPs at this concentration slightly enhanced plant growth (10,11).
99 Each treatment had 12 replicates. The solutions in the jars were replenished every other
100 day with the same treatment solution to compensate for evapotranspiration, with the
101 assumption that Ce would be taken up concurrently with water by plants. However, if
102 plants preferably take up water, it is possible that cerium would accumulate in the
103 growing solution. Plants were harvested 35 days after germination (i.e., 21 days after
104 treatment). Additionally, a separate set of radish plants were grown and treated exactly as
105 above. The harvested tissues from these plants were used to determine the distribution of
106 cerium across the fine root tips and storage roots microscopically (see below for details).

107 **Plant physiological responses**

108 For the first batch of plants, daily transpiration rate was recorded for each
109 seedling after they were transferred to 100 mL glass jars by measuring the water surface
110 drop before the solution replenishment. The cumulative transpiration of each treatment
111 was then calculated by summing the daily transpiration over the 21 d treatment period.
112 Relative chlorophyll content was measured with a SPAD 502 Plus Chlorophyll Meter
113 (Spectrum Technologies, Inc. Aurora, IL) one day prior to harvest and was expressed as a
114 percent of control. An OS1p chlorophyll fluorometer (Opti-sciences, Inc. Hudson, NH)
115 was used to measure the yield of quantum efficiency of PSII (light-adapted Y(II)) and the
116 photochemical efficiency of PSII (dark-adapted F_v/F_M) on the same day the relative
117 chlorophyll was measured. Five of the 12 replicates from each treatment were used in a
118 leakage test to assess root membrane integrity. The leakage test followed the published

119 procedures with some modifications (19). Briefly, the entire fine root system was
120 submerged in 50 mL of deionized water and the initial conductivity C_w was measured
121 immediately (Orion ROSS Ultra pH/ATC Triode Orion Star A325 Thermo Fisher
122 Scientific, Waltham, MA). The conductivity of the solution was measured again as C_0
123 after 3 hours of incubation at room temperature. The entire fine roots were then
124 autoclaved at 121°C for 20 min with a Tuttnauer Brinkman 3850M autoclave to release
125 all electrolytes. The final conductivity C_t was measured after the samples cooled to room
126 temperature. The percentage of electrolyte leakage was calculated as: $EL = (C_0 - C_w) / (C_t -$
127 $C_w) \times 100$.

128 **Uptake, accumulation and distribution of cerium**

129 At harvest, radish plants were separated into fine roots, storage roots (the edible
130 radish bulb), and shoots. The tissues were then dried in an oven at 75 °C for 7 days and
131 their dry weights determined. For each treatment, the 12 storage roots and 12 shoot
132 tissues were divided into to four groups respectively. The shoot and storage root tissues
133 in each group were then ground together into fine powders, from which 0.25 g of the
134 ground tissues were weighed and digested in 4 mL of 70% nitric acid and swirled to mix.
135 For the fine roots, the remaining seven replicates (five replicates used for the electrolyte
136 leakage test were excluded) were divided into three groups and each group contained
137 either two or three of the fine root systems. Due to the smaller biomass of the fine roots,
138 all ground tissues from each group were used for the digestion. The nitric acid digest was
139 heated at 95 °C for 20 minutes and then 45 °C for 4 minutes, and the cycle was repeated
140 5 times until all the dry tissues were dissolved. Afterwards, 2 mL of hydrogen peroxide
141 was added to the mixture and heated using the same temperature cycle until the solution

142 was clear. The digest solution was then analyzed by inductively coupled plasma – mass
143 spectrometry (ICP-MS) to obtain the concentration of cerium in each sample.

144 The radish roots used to determine the localization and distribution of cerium in
145 their fine roots and storage roots were harvested at day 21 after treatment. To obtain a
146 reference for the anatomy of the radish storage root, a cross section of the radish storage
147 root taken at the equator was cut with a razor blade and observed under a Kruss
148 MBL3000 light microscope (A.KRÜSS Optronic, Hamburg, Germany) (Supplementary
149 Figure 1). The radish fine root tips and sections of the storage roots from each treatment
150 were also examined using a Zeiss LSM 510 META confocal microscope. A laser
151 excitation wavelength of 543 nm was used and an emission filter band pass was set
152 between 530-590 nm to collect both the laser reflection and autofluorescence in this
153 region. To image the storage root, the root was first cut in half horizontally from the
154 thickest point and then a thin slice (~ 1mm) of the storage root was cut from the bottom
155 half of the storage root. That slice was then divided into four quarters and one of the
156 quarters was randomly selected to determine the radial distribution of cerium toward the
157 midpoint of the storage root. A schematic illustration of the slices preparation is shown in
158 Supplementary Figure 1. For each sample, a serial scanning along the z-axis of the
159 sample was conducted and the numbers of scanning planes varied from 8 to 11. The
160 distance between two optical planes was approximately 10.2 μm .

161 **Data Analysis**

162 A one-way ANOVA was performed in this study for data analysis. The Duncan
163 test was conducted for post hoc comparisons.

164

165 **Results**

166 **Characterization of CeO₂ NPs and the bulk**

167 Supplementary Figure 2 shows the TEM images of CeO₂ NPs and bulk CeO₂ in
168 quarter strength Hoagland solution. The nanoparticles displayed variable shapes and
169 sizes. Individual nanoparticles possessed triangular, rectangular and other irregular
170 shapes. The images indicate that the average diameter of individual CeO₂ NPs ranged
171 from 10 – 30 nm. The nanoparticles aggregated considerably in the Hoagland solution,
172 due to the high ionic strength. The hydrodynamic diameter of the nanoparticle aggregates
173 was ~600 nm as measured by the DLS. The zeta potential of CeO₂ NPs in the Hoagland
174 solution was approximately -11.9 mV, suggesting that the nanoparticles were not stable.
175 Bulk CeO₂ were mostly at the micron scale but the sizes were not uniform. Particles at
176 the nanoscale were also detected in the bulk solutions. The sizes of bulk CeO₂ ranged
177 approximately from 100 nm to 4,000 nm.

178 **Plant physiological status**

179 The radish exposed to CeO₂ bulk had the highest total dry biomass and was
180 significantly greater than all other treatments (Figure 1a). The biomass of the
181 nanoparticle treated plants was not significantly different from the control plants. The
182 plant biomass exposed to cerium ions was significantly lower than all other treatments.
183 When the plant tissues were examined separately, the bulk cerium treated radishes, which
184 had similar shoot biomasses as CeO₂ NPs-treated radishes, had significantly higher dry
185 shoot biomass than control and cerium ions treatment (Figure 1b). The dry weight of
186 storage roots across the treatments exhibited similar patterns as the total dry biomass
187 (Figure 1c), but the dry biomass of fine roots did not differ significantly as a function of

188 treatment (Figure 1d). In addition to the total biomass, the distribution of the biomass
189 between the root (fine + storage root) and shoot compartments was significantly different
190 in response to treatment. The shoot/root ratio of dry biomass of cerium ion treated radish
191 (1.34 ± 0.11) was significantly higher ($p < 0.05$) than all other treatments, which had
192 similar ratios (control: 1.00 ± 0.10 ; bulk CeO₂: 0.95 ± 0.06 ; CeO₂ NPs: 1.07 ± 0.07).
193 Visually, there was no apparent adverse effect of any of the cerium treatments on growth
194 and development of the radish plants except for the size differences (Figure 1e).

195 In addition to the root biomass, the fine root membrane integrity was significantly
196 affected by different forms of cerium. Figure 2 indicates that 10 mg/L of CeO₂ NPs and
197 ionic cerium resulted in significantly greater electrolyte leakage when compared to the
198 control roots. Leakage from bulk cerium treated roots was not significantly different from
199 control roots. The accumulative transpiration of radish for all treatments was comparable
200 until day 21, since then the accumulative transpiration of cerium ion treated radish
201 became significantly lower than other treatment groups (Supplementary Figure 3). The
202 relative chlorophyll content expressed in percentage is shown in Table 1. Although all
203 treated radishes had lower chlorophyll content, only the bulk CeO₂ and CeO₂ NPs treated
204 leaves had significantly lower chlorophyll content compared to the controls. The average
205 quantum yield of photosystem II (Y(II)) and the F_v/F_m ratio for plants from different
206 treatments are also shown in Table 1. The results indicated that the Y(II) was unaffected
207 by the treatments. In contrast, only bulk CeO₂ treated radishes displayed an F_v/F_m ratio
208 significantly lower value than the control. No significant differences were observed
209 between the other cerium treatments.

210 **Cerium uptake and accumulation**

211 Not surprisingly, exposure to cerium resulted in significantly greater
212 concentrations of this element in plant tissues. For the treated plants, the cerium
213 concentration and content were significantly higher in the fine roots than in other tissues
214 (Figure 3a-d). Among different treatments, the concentration of cerium in the storage root
215 was not significantly different between cerium treatments (Figure 3a). In the shoot
216 tissues, cerium ion treated radish had highest cerium concentration, followed by bulk
217 cerium and then CeO₂ NPs treated radish (Figure 3a). The fine roots of CeO₂ NPs treated
218 radish had significantly higher concentration of cerium than the bulk and ion treated
219 radish (Figure 3b). When the cerium content rather than the concentration in different
220 tissues was compared, cerium content in the storage roots of different treatments was still
221 similar. The shoot cerium content of bulk and ion treated radishes was not significantly
222 different but was markedly higher than nanoparticle treated radishes (Figure 3c). In the
223 fine roots, the cerium content demonstrated similar patterns as the cerium concentration
224 for different treatments (Figure 3d).

225 **Cerium localization and distribution in radish root and storage root**

226 For the fine root tips, the confocal microscopic images were captured both on the
227 surface and at different depths from the surface. The control had some weak signals from
228 either the cerium content in control tissues or from background excitation (Figure 4a). In
229 contrast, plant roots from treated plants all generated stronger signals (Figure 4b-f).
230 However, the signal patterns were noticeably different. On the bulk CeO₂ treated root, the
231 signals were only detected from the mucilage surrounding the root tip in both surface and
232 deeper scanning images (Figure 4b,c). CeO₂ NPs were detected on larger areas of the root
233 surface as well as the mucilage on the root tip of the nanoparticle treated plants (Figure

234 4d). The signal was even more prominent in the deeper scanning planes (Figure 4e). For
235 cerium ion treated radish root, the signals were predominantly detected in the
236 surrounding areas. Neither the surface scan nor the deep scan detected significantly
237 stronger signals than the controls within the root itself (Figure 4f).

238 Figure 5 shows the confocal images of cut slices of radish storage roots. The
239 control storage root showed little signal (Figure 5a). In comparison, storage roots from
240 treated plants had strong signals. For bulk CeO₂ treated radish, all signals came from the
241 pigmented periderm with a random pattern (Figure 5b). For CeO₂ NPs treated radish,
242 stronger signals were observed in the pigmented periderm. In addition, the nanoparticles
243 appeared to penetrate further into the storage root (Figure 5c). Cerium was not only
244 detected in the periderm but also in the secondary vascular tissues in the storage root of
245 cerium ion treated radish (Figure 5d,e).

246

247 **Discussion**

248 Accompanied with the ever expanding applications of engineered nanomaterials
249 are the increasing concerns about their toxicity to humans and the environment. A major
250 question scientists are trying to ascertain is whether the reduction of micro-sized particles
251 to nano-sized particles will significantly increase their toxicity. Several previous studies
252 have shown that nanoparticles typically exhibit stronger effect on plants than their bulk
253 counterparts (20, 21). For example, following a 15-day hydroponic exposure, the biomass
254 of zucchini plant exposed to silver nanoparticles was 75% less than plants treated with
255 same concentrations of bulk silver powder (21). For CeO₂ particles, it is well accepted
256 that the presence of highly mobile lattice oxygen on the surface will cause oxygen

257 vacancy on the surface (22). With the decrease of nanoparticle size, the specific surface
258 area and consequently the density of the oxygen vacancy increase. The separation of
259 oxygen from the lattice structure generates electrons which can be used to reduce Ce^{4+} to
260 Ce^{3+} . With increasing oxygen vacancy, the ratio of Ce^{3+}/Ce^{4+} will increase on the surface
261 of nanoparticles (23). Because Ce^{3+} is about 14% larger than Ce^{4+} (22), the conversion of
262 Ce^{4+} to Ce^{3+} will strain the lattice structure and increase the reactivity and the superoxide
263 dismutase (SOD) mimetic activity of the CeO_2 particles (24). Therefore, particle size is
264 an important consideration in the assessment of the environmental toxicity of CeO_2 .
265 Unfortunately, information on the size effect of CeO_2 particles on plant development in
266 the literature is very limited.

267 Due to the potential dissolution of some metallic nanoparticles, another major
268 question actively investigated in the scientific community of nanotoxicology is the
269 comparative toxicity of nanoparticles and the ionic form of the particles. Because of the
270 general acceptance that CeO_2 NPs are stable in liquid solutions, ionic cerium was
271 generally not included in the treatment paradigms (13-16). However, the broad
272 applications of different forms and sizes of cerium require a comprehensive
273 understanding and comparison of their fate and phytotoxicity. Our investigation provides
274 an assessment of the differential fate and phytotoxicity of cerium in its ionic, nanoscale
275 and bulk particle forms. Several physiological parameters including the root membrane
276 integrity photosynthesis-related measurements, and biomass parameters were affected by
277 certain forms of cerium at the tested concentration.

278 While the specific mechanisms by which cerium compounds may compromise
279 membrane integrity are not known and may differ, all forms and sizes of cerium resulted

280 in some damage to root membrane integrity as indicated by an increase in electrolyte
281 leakage. The effect was significant however only for the nanoparticle and ionic forms.
282 The changes in the integrity of root membrane could also alter the membrane potential
283 and potentially the function of the membrane (24). It has been reported that altered
284 plasma membrane integrity and potential is associated with changes in the ion fluxes into
285 plant roots (25). Whether this alteration of membrane integrity influenced the
286 concentration of any essential macronutrients or micronutrients in radish was not
287 examined but would be a reasonable question for future studies. For the bulk CeO₂ and
288 CeO₂ NPs, in addition to their impact on the membrane, physical adsorption on root
289 surface and blockage of nutrient uptake by plant roots may also occur. It is possible that
290 such impacts on the roots may have affected the uptake of elements such as magnesium
291 or iron, two nutrients associated with the synthesis of chlorophyll. A decrease in the
292 concentration of either of these essential nutrients might have contributed to the decrease
293 in relative chlorophyll content observed in some treatments. Other aspects of chlorophyll
294 synthesis or degradation could have been affected as well and a more detailed study will
295 be required to understand the extent or severity of effects of cerium on chlorophyll
296 metabolism. The significantly lower F_v/F_M values observed for the bulk cerium treatment
297 as compared to the control plants suggested that photosynthetic electron transport
298 associated with photosystem II was stressed in those plants, but not for the other cerium
299 treatments. These results differ from a study with plantlets of *Medicago arborea* in
300 which nanoceria was found to have a more negative effect on the F_v/F_M ratio than the
301 same concentrations of bulk cerium (25). Other studies have shown that the influence of
302 cerium compounds on plant photochemistry differs depending on factors such as plant

303 Mn status (26,) and the presence of salt stress (27). Definitive conclusions about the
304 comparative phytotoxicity of the cerium ion and nanoceria cannot be made without
305 further investigation. Even so, the overall effect of all treatments on the two
306 photosynthetic parameters measured were modest and perhaps not indicative of a
307 significant stress imposed on the plants, particularly given that there were no overt visible
308 effects observed for any treatments, including the ionic cerium and the CeO₂ NPs
309 treatments. The only other indication of a negative effect of treatment with cerium was
310 the decrease in biomass observed for the cerium ion treatment.

311 The shoot/root ratio of radish was also affected by cerium, primarily through the
312 change of the biomass of the storage roots. Because the root thickening is a result of the
313 combined cell division and enlargement of secondary xylem and phloem cells which
314 depends on the activity of the vascular cambium (28), it is possible that the cerium of
315 different forms have different impacts on the activity of the vascular cambium. One could
316 speculate that the bulk CeO₂ might have enhanced the activity of the vascular cambium
317 while ionic Ce inhibited it. Metabolically, according to the “sink capacity” theory, the
318 storage root represents a major reservoir for radish and sucrose transported within radish
319 is the main carbohydrate for the growth of sinks. As such, photosynthate distribution into
320 different tissues is heavily affected by the activity of sucrose synthase (SuSy) (29-32). If
321 future studies examined the expression of SuSy genes and/or measured the activity of this
322 enzyme in the radish hypocotyl in response to different forms of cerium, it might be
323 possible to ascertain whether the changes in the mass of the storage root in response to
324 bulk or ionic cerium treated radish plants were due to changes in sink strength. The
325 specific mechanisms by which these cerium compounds influence the biomass of radish

326 storage roots has implications for the agricultural production of radish and related
327 vegetable species and are therefore worth further attention.

328 It should be pointed out that concentration of CeCl_3 used in this study was very
329 low and the impact of chloride ion is not expected to be substantial. Parida and Das (33)
330 investigated plant salt tolerance and salinity effects on plant growth and the authors
331 reported that under 100 mM NaCl (3.55 g/L Cl^-), chloride demonstrated limited influence
332 on the osmotic adjustment of cell membrane. Scialabba and Melati (34) also reported that
333 sodium chloride up to a concentration of 0.1% positively affected radish growth. The Cl^-
334 in the ionic cerium solution used in this study was significantly lower than those reported
335 values and was not expected to significantly contribute to the negative effect observed in
336 the ionic treatment group. Consequently, the negative effect observed in the ionic
337 treatment should be attributed to the ionic cerium. Another caveat about the results is that
338 10 mg/L was the concentration of the compounds of CeO_2 and CeCl_3 , not the
339 concentration of cerium as an element. Due to the different molecular weight percentage
340 of cerium in CeO_2 and CeCl_3 , the actual concentration of cerium as an element was 8.14
341 mg Ce/L in CeO_2 NPs and the bulk and was only 5.68 mg Ce/L in the ionic form. Cerium
342 in CeO_2 was 43.5% higher than in the ionic form. If the equivalent concentration of
343 cerium as an element was used, the ionic cerium may display an even stronger effect on
344 plant physiology.

345 In addition to the yield of edible storage root, the potential accumulation of
346 cerium was examined. Exposed plants had detectable cerium in all plant tissues,
347 including the edible storage roots and leaves even though the forms of cerium in these
348 tissues are unknown. However, the forms of cerium in plant tissues may affect both their

349 toxicity and potential availability to humans and they deserve detailed investigation in
350 future studies. In current study, the significantly higher cerium detected in the shoot
351 tissues of exposed plants indicated that cerium translocation from roots to shoot had
352 occurred. The upward transport of bulk cerium to radish shoots was unexpected given the
353 size of the particles and the low dissolution rate of bulk CeO₂. It is most likely that the
354 cerium content detected from the bulk treated shoot tissues was from the nanoscale
355 particles present in the bulk mixture (Supplementary Figure 2). The upward transport of
356 CeO₂ NPs and ionic cerium from roots to shoots was expected and has been reported in
357 the literature (10, 14, 35). Interestingly, however, when the cerium localization in the
358 storage root was investigated with the confocal microscope, signals of cerium in the
359 vascular tissues were only observed in cerium ion treatment, suggesting that active
360 transport may function as an important pathway of cerium accumulation only for ion
361 treated radishes. In contrast, signals from the CeO₂ NPs and bulk treated radish roots
362 were mainly located on the periderms. The results suggest that adsorption and diffusion
363 of particulate cerium along the radial direction might be a more important pathway for
364 CeO₂ NPs and bulk accumulation in radish storage roots. The diffusion may possibly
365 occur from the lenticels on the periderm, but more precise techniques are needed to
366 confirm this assumption. From the food safety point of view, the cerium accumulation in
367 the edible storage root is more concerning and our results showed that while cerium
368 concentration and content were similar across the cerium treatment, the distribution of
369 cerium in the storage roots varied and consequently their availability to humans would
370 vary. For example, the majority of particulate cerium accumulated in the edible tissue
371 could be removed in the food preparation process while ionic cerium in the storage roots

372 is more likely to be consumed by humans with the storage root.

373 In closing, our results suggested that 10 mg/L cerium as cerium oxide or cerium
374 chloride could affect the growth of radish and could accumulate in the edible storage root
375 and shoot tissues. However, the impact and accumulation patterns varied significantly by
376 the size and chemical form of cerium. Ionic cerium displayed the strongest impact on
377 radish root membrane integrity and growth, followed by CeO₂ NPs and then the bulk.
378 While cerium of different forms all accumulate in radish tissues, their accumulation
379 potential and distribution patterns varied greatly. As a result, potential exposure and risk
380 to human health through diet exposure to different sizes and forms of cerium may vary
381 and these differences should be considered when evaluating the food safety of cerium in
382 the environment.

383

384 **Acknowledgement**

385 The authors acknowledge the financial support of the USDA-AFRI (#2012-67005-19585)
386 and USDA-AFRI (#2011-67006-30181).

387

388 **Supporting Information Available**

389 The transmission electron microscopic images of bulk CeO₂ and CeO₂ NPs, the
390 accumulative transpiration of radish plants and the anatomy of radish storage root were
391 provided as supporting information. This information is available free of charge via the
392 Internet at <http://pubs.acs.org>.

393

394

395 **References**

- 396 (1) Tiede, K.; Hassellöv, M.; Breitbarth, E.; Chaudhry, Q.; Boxall, A., Considerations for
397 Environmental Fate and Ecotoxicity Testing to Support Environmental Risk
398 Assessments for Engineered Nanoparticles. *J. Chromatogr. A.* **2009**, *1216*(3), 503-
399 509.
- 400 (2) Nowack, B.; Bucheli, T. D., Occurrence, Behavior and Effects of Nanoparticles in the
401 Environment. *Environ. Pollut.* **2007**, *150*(1), 5-22.
- 402 (3) Bystrzejewska-Piotrowska, G.; Golimowski, J.; Urban, P. L., Nanoparticles: Their
403 Potential Toxicity, Waste and Environmental Management. *Waste Manage.* **2009**,
404 *29*(9), 2587-2595.
- 405 (4) Brar, K.; Verma, M.; Tyagi, R. D.; Surampalli, R. Y. Engineered Nanoparticles in
406 Wastewater and Wastewater Sludge – Evidence and Impacts. *Waste Manage.* **2010**,
407 *30*(3), 504-520.
- 408 (5) Been, T. M.; Westerhoff, P. Nanoparticle Silver Released into Water from
409 Commercially Available Sock Fabrics. *Environ. Sci. Technol.* **2008**, *42*(11), 4133–
410 4139.
- 411 (6) Limbach, L. K.; Bereiter, R.; Müller, E.; Krebs, R.; Gälli, R.; Stark, W. J. Removal of
412 Oxide Nanoparticles in a Model Wastewater Treatment Plant: Influence of
413 Agglomeration and Surfactants on Clearing Efficiency. *Environ. Sci. Technol.* **2008**,
414 *42*(15), 5828–5833.
- 415 (7) Pelletier, D. A.; Suresh, A. K.; Holton, G. A.; McKeown, C. K.; Wang, W.; Gu, B.;
416 Mortensen, N. P.; Allison, D. P.; Joy, D. C.; Allison, M. R.; Brown, S. D.; Phelps, T.
417 J.; Doktycz, M. J. Effects of Engineered Cerium Oxide Nanoparticles on Bacterial
418 Growth and Viability. *Appl. Environ. Microbiol.* **2010**, *76*(24), 7981-7989.
- 419 (8) Rosenkranz, P.; Fernández-Cruz, M. L.; Conde, E.; Ramírez-Fernández, M. B.;
420 Flores, J. C.; Fernández, M.; Navas, J. M. Effects of Cerium Oxide Nanoparticles to
421 Fish and Mammalian Cell Lines: An Assessment of Cytotoxicity and Methodology.
422 *Toxicol. in Vitro.* **2012**, *26*(6), 888-896.
- 423 (9) Zhu, H.; Han, J.; Xiao, J. Q.; Jin, Y. Uptake, Translocation, and Accumulation of
424 Manufactured Iron Oxide Nanoparticles by Pumpkin Plants. *J. Environ. Monit.* **2008**,
425 *10*(6), 713–717.
- 426 (10) Wang, Q.; Ma, X.; Zhang, W.; Pei, H.; Chen, Y. The Impact of Cerium Oxide
427 Nanoparticles on Tomato (*Solanum Lycopersicum* L.) and Its Implications for Food
428 Safety. *Metallomics.* **2012**, *4*(10), 1105-1112.
- 429 (11) Wang, Q.; Ebbs, S. D.; Chen, Y.; Ma, X. Trans-generational Impact of Cerium
430 Oxide Nanoparticles on Tomato Plants. *Metallomics.* **2013**, *5*(6), 753-759.

- 431 (12) Ma, Y.; Kuang, L.; He, X.; Bai, W.; Ding, Y.; Zhang Z.; Zhao, Y.; Chai, Z. Effects
432 of Rare Earth Oxide Nanoparticles on Root Elongation of Plants. *Chemosphere*. **2010**,
433 78(3), 273–279.
- 434 (13) Rico, C. M.; Hong J.; Morales, M. I.; Zhao, L.; Barrios, A. C.; Zhang, J. Y.;
435 Peralta-Videa, J. R.; Gardea-Torresdey, J. L. Effect of Cerium Oxide Nanoparticles on
436 Rice: A Study Involving the Antioxidant Defense System and In Vivo Fluorescence
437 Imaging. *Environ. Sci. Technol.* **2013**, 47(11), 5635-5642.
- 438 (14) Zhang, Z.; He, X.; Zhang, H.; Ma, Y.; Zhang, P.; Ding, Y.; Zhao, Y. Uptake and
439 Distribution of Ceria Nanoparticles in Cucumber Plants. *Metallomics*. **2011**, 3(8),
440 816-822.
- 441 (15) Zhao, L.; Peralta-Videa, J. R.; Varela-Ramirez, A.; Castillo-Michel, H.; Li, C.;
442 Zhang, J.; Aguilera, R. J.; Keller, A. A.; Gardea-Torresdey, J. L. Effect of Surface
443 Coating and Organic Matter on the Uptake of CeO₂ NPs by Corn Plants Grown in
444 Soil: Insight Into the Uptake Mechanism. *J. Hazard Mater.* **2012**, 225, 131-138.
- 445 (16) Lopez-Moreno, M. L.; de la Rosa, G.; Hernandez-Viezcas, J.; Castillo-Michel, H.;
446 Botez, C.; Peralta-Videa, J. R.; Gardea-Torresdey, J. L. Evidence of the Differential
447 Biotransformation and Genotoxicity of ZnO and CeO₂ Nanoparticles on Soybean
448 (*Glycine max*) Plants. *Environ. Sci. Technol.* **2010**, 44(19), 7315-7320.
- 449 (17) Boxall, A., Chaudhry, Q., Sinclair, C., Jones, A., Aitken, R., Jefferson, B., Watts,
450 C. *Current and Future Predicted Environmental Exposure to Engineered*
451 *Nanoparticles*. Central Science Laboratory, Department of the Environment and
452 Rural Affairs, London, UK. **2007**.
- 453 (18) Sanchez-Viveros, G.; Gonzalez-Mendoza, D.; Alarcon, A.; Ferrera-Cerrato, R.
454 Copper Effects on Photosynthetic Activity and Membrane Leakage of *Azolla*
455 *Filiculoides* and *A. Caroliniana*. *Int. J. Agr. Biol.* **2010**, 12(3), 365-368.
- 456 (19) Feizi, H., Moghaddam, P. R., Shahtahmassebi, N., Fotovat, A. Impact of bulk and
457 nanosized titanium dioxide (TiO₂) on wheat seed germination and seedling growth.
458 *Biol. Trace Elem. Res.* **2012**, 146(1), 101-106.
- 459 (20) Stampoulis, D., Sinha, S. K., White, J. C. Assay-dependent phytotoxicity of
460 nanoparticles to plants. *Environ. Sci. Technol.* **2009**, 43(24), 9473-9479.
- 461 (21) Dutta, P., Pal, S., Seehra, M. S., Shi, Y., Eyring, M., Ernst, R. D. Concentration of
462 Ce³⁺ and oxygen vacancies in cerium oxide nanoparticles. *Chem. Mater.* **2006**, 18,
463 5144-5146.
- 464 (22) Deshpande, S., Patil, S., Kuchibhatla, S. T., Seal, S. Size Dependency Variation in
465 Lattice Parameter and Valency States in Nanocrystalline Cerium Oxide. *Appl. Phys.*
466 *Lett.* **2005**, 87(13), 133113
- 467 (23) Heckert, E. G., Karakoti, A. S., Seal, S., Self, W. T. The Role of Cerium Oxide

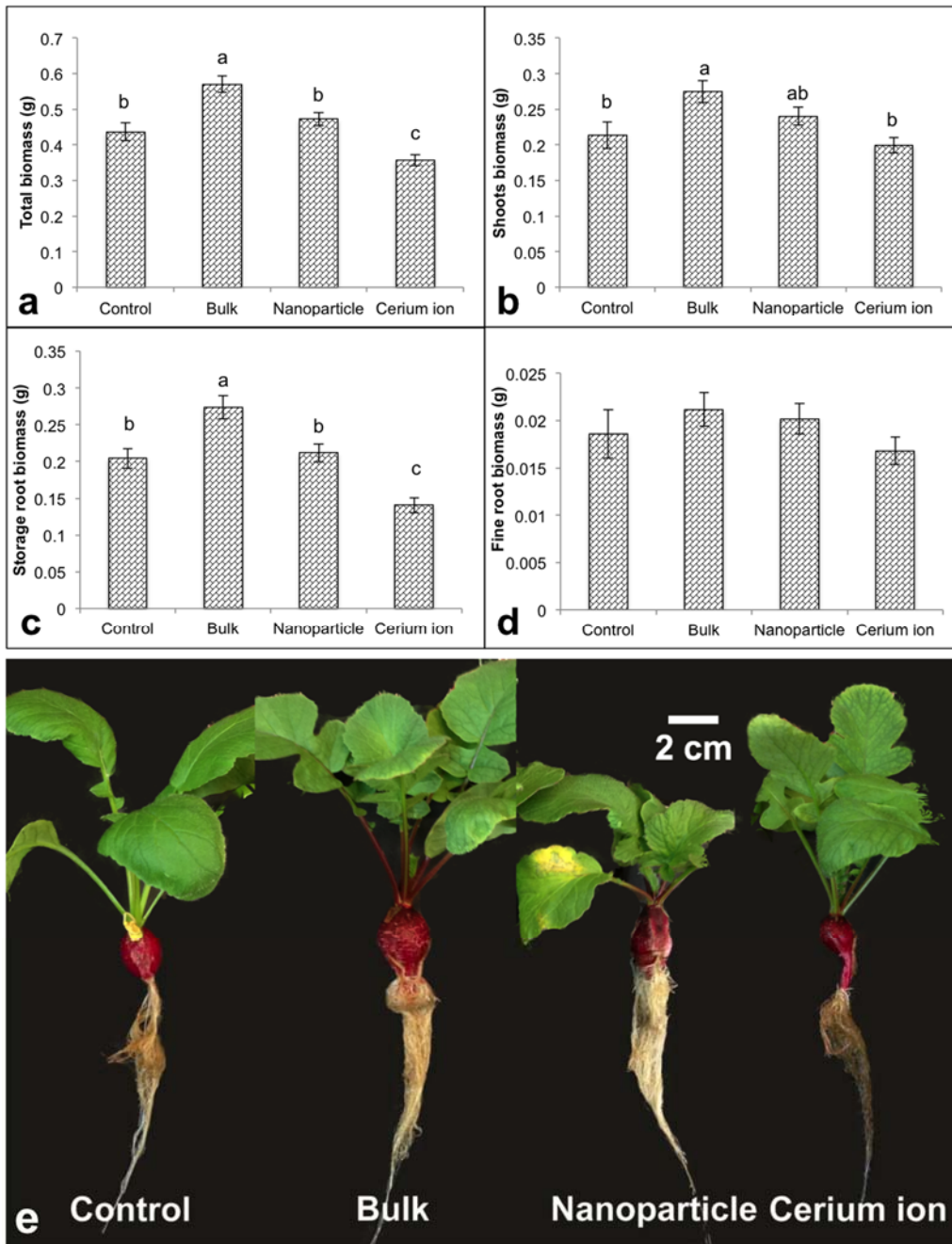
- 468 State in the SOD Mimetic Activity of Nanoceria. *Biomaterials*. **2008**, 29(18), 2705-
469 2709.
- 470 (24) Lindberg, S., Strid, H. Aluminium Induces Rapid Changes in Cytoplasmic pH and
471 Free Calcium and Potassium Concentrations in Root Protoplast of Wheat (*Triticum*
472 *aestivum*). *Physiol. Plantarum*. **1997**, 99(3), 405-414.
- 473 (25) Gomez-Garay, A., Pintos, B., Manzanera, J. A., Lobo, C., Villalobos, N., Martin,
474 L. Uptake of CeO₂ Nanoparticles and Its Effect on Growth of *Medicago arborea* in
475 Vitro Plantlets. *Biol. Trace. Elem. Res.*, **2014**, 161, 143-150,
- 476 (26) Qu, C., Liu, C., Guo, F., Hu, C., Ze, Y., Li, C., Zhou, Q., Hong, F. Improvement of
477 Cerium on Photosynthesis of Maize Seedlings Under a Combination of Potassium
478 Deficiency and Salt Stress. *Biol. Trace. Elem. Res.*, **2014**, 155, 104-113.
- 479 (27) Qu, C., Gong, X., Liu, C., Hong, M., Wang, L., Hong, F. Effects of Manganese
480 Deficiency and Added Cerium on Photochemical Efficiency of Maize Chloroplasts.
481 *Biol. Trace. Elem. Res.*, **2012**, 146, 94-100.
- 482 (28) Wherrett, T., Ryan, P. R., Delhaize, E., Shabala, S. Effect of Aluminum on
483 Membrane Potential and Ion Fluxes at the Apices of Wheat Roots. *Funct. Plant Biol.*
484 **2005**, 32(3), 199-208.
- 485 (29) Zaki, H. E. M., Takahata, Y., Yokoi, S. Analysis of the Morphological and
486 Anatomical Characteristics of Roots in Three Radish (*Raphanus sativus*) Cultivars
487 that Differ in Root Shape. *J. Hortic. Sci. Biotech.* **2012**, 87(2), 172-178.
- 488 (30) Farrar, J. F. Regulation of Shoot-root Ratio is Mediated by Sucrose. *Plant Soil.*
489 **1996**, 185(1), 13-19.
- 490 (31) Rouhier, H.; Usuda, H. Spatial and Temporal Distribution of Sucrose Synthase in
491 the Radish Hypocotyl in Relation to Thickening Growth. *Plant cell physiol.* **2001**,
492 42(6), 583-593.
- 493 (32) Usuda, H.; Demura, T.; Shimogawara, K.; Fukuda, H. Development of Sink
494 Capacity of the "Storage Root" in a Radish Cultivar with a High Ratio of "Storage
495 Root" to Shoot. *Plant Cell Physiol.* **1999**, 40(4), 369-377.
- 496 (33) Wardlaw, I. F. The Control and Pattern of Movement of Carbohydrates in Plants.
497 *Bot. Rev.* **1968**, 34(1), 79-105.
- 498 (34) Parida, A. K.; Das, A. B. Salt Tolerance and Salinity Effects on Plants: A Review.
499 *Ecotox. Environ. Safe.* **2005**, 60(3), 324-349.
- 500 (35) Scialabba, A.; Melati, M. R. The Effect of NaCl on Growth and Xylem
501 Differentiation of Radish Seedlings. *Bot. Gaz.* **1990**, 151(4), 516-521.
- 502 (36) Hu, X., Ding, Z., Chen, Y., Wang, X., Dai, L. Bioaccumulation of Lanthanum and

503 Cerium and Their Effects on the Growth of Wheat (*Triticum aestivum L.*) Seedlings.
504 *Chemosphere*. **2002**, 48(6), 621-629.
505
506
507
508
509
510
511
512
513
514
515
516
517
518
519
520
521
522
523
524
525
526
527
528
529
530
531
532
533
534
535
536
537
538
539
540
541
542
543
544
545
546
547

548 **Table 1:** The relative chlorophyll content expressed as percentage of control of each
 549 treatment, the average Y(II), F_v/F_M ratio, n=12. Different letters in the table represent
 550 significant differences between the treatments (p<0.05).
 551

Treatment	Relative Chlorophyll (%)	Standard error	Y(II)	Standard error	F _v /F _M	Standard error
Control	100.00 ^a	2.67	0.774	0.007	0.830 ^a	0.003
Bulk	87.22 ^b	3.84	0.728	0.022	0.757 ^b	0.026
Nanoparticle	83.69 ^b	4.24	0.731	0.020	0.780 ^{ab}	0.016
Cerium ion	91.51 ^{ab}	4.68	0.697	0.060	0.797 ^{ab}	0.020

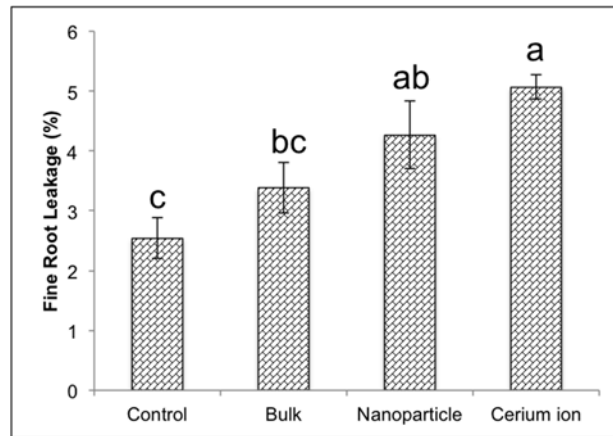
552
 553
 554
 555
 556
 557
 558
 559
 560
 561
 562
 563
 564
 565
 566
 567
 568
 569
 570
 571
 572
 573
 574
 575
 576
 577
 578
 579
 580
 581
 582
 583
 584
 585
 586
 587



589
 590
 591
 592
 593
 594
 595
 596
 597
 598
 599

Figure 1: Dry biomass of total radish and different radish tissues treated with 10 mg/L of different forms of cerium (a-d). The reported values are the mean of 12 replicates and the error bars represent standard error. Different letters represent significant differences between the treatments ($p < 0.05$). (e) Images of typical radish plants from the different treatments.

600



601

602

603 **Figure 2:** Electrolyte leakage from radish fine roots grown hydroponically in different

604 solutions. The reported values are the average of 5 replicates in each treatment and the

605 error bars represent standard error. Different letters represent significant differences

606 between the treatments ($p < 0.05$).

607

608

609

610

611

612

613

614

615

616

617

618

619

620

621

622

623

624

625

626

627

628

629

630

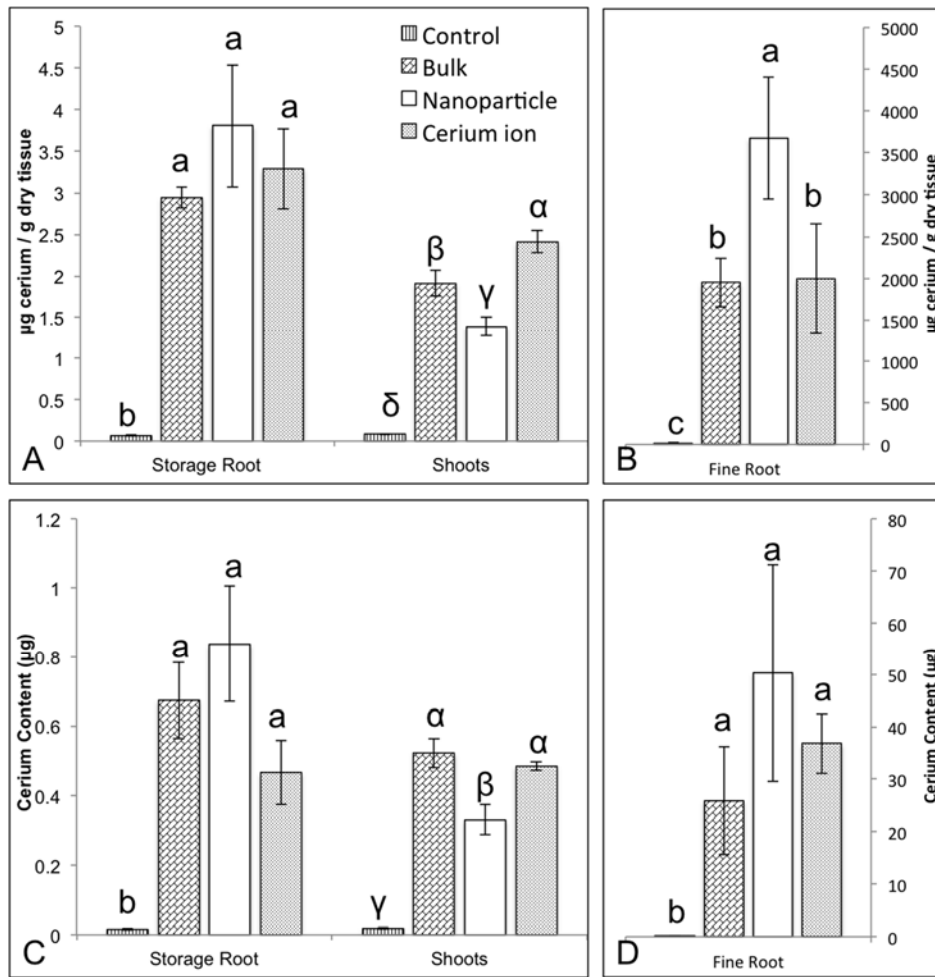
631

632

633

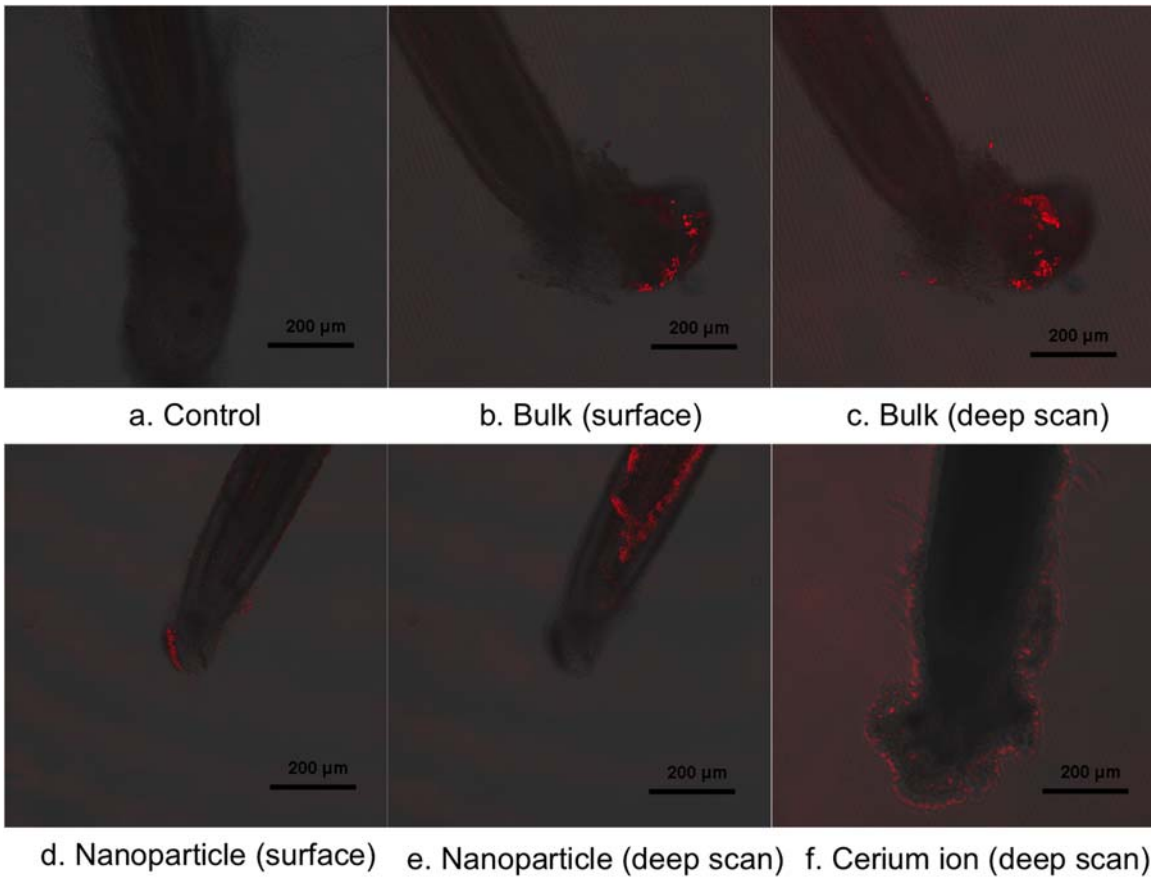
634

635



636
637
638
639
640
641
642
643
644
645
646
647
648
649
650

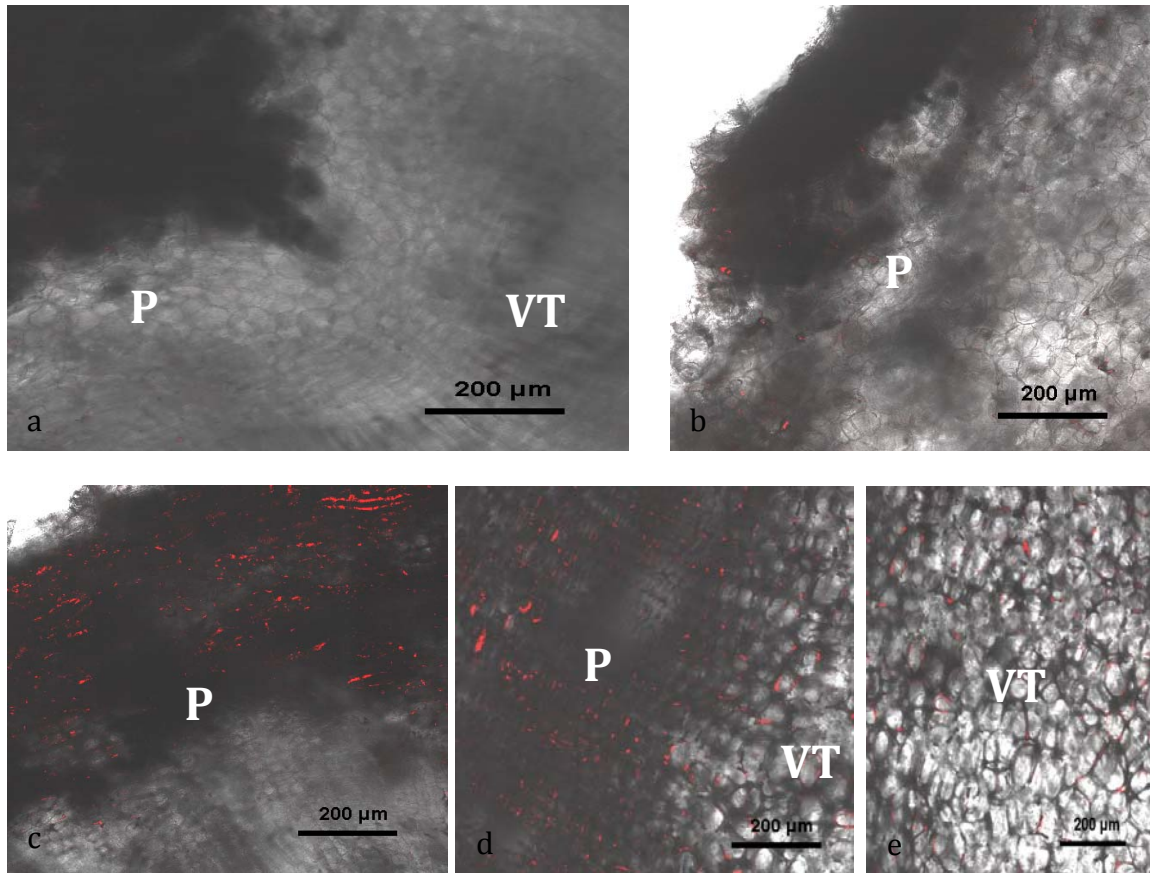
Figure 3: Cerium concentration (A and B) and mass (C and D) in different radish tissues. The reported values in A and C are the average of 4 measurements. The reported values in B and D are the average of 2 or 3 measurements. Errors bars represent standard error. Letters above bars reflect their statistical grouping. Different letters and Greek symbols represent significant differences between the treatments ($p < 0.05$).



651
652
653
654
655
656
657
658
659
660
661
662
663
664
665
666
667
668
669
670
671
672
673
674

Figure 4: Confocal microscopic images depicting the accumulation of cerium in the fine roots of radish. (a) control root showing weak signals, (b, c) surface and representative deeper scan of fine roots treated by bulk CeO₂, (d, e) surface and representative deeper scan of fine roots exposed to CeO₂ NPs and (f) a deeper scan image of fine roots exposed to cerium ion. The deeper scan images shown were selected from a stack of deep scan images for different roots.

675



676

677

678

679

680

681

682

683

684

685

686

687

688

689

690

691

692

693

694

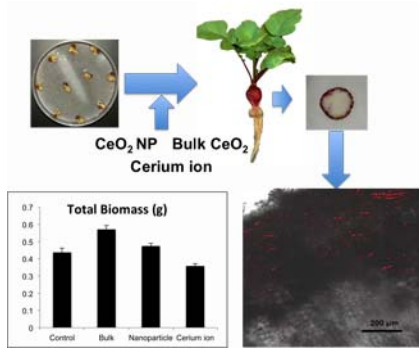
695

696

Figure 5: (a) Confocal images of the horizontal slices of radish storage root treated with different types of cerium. (a): control; (b): bulk CeO₂ treated radish; (c): CeO₂ NPs treated radish and (d, e): ionic cerium treated radish. P: Periderm; VT: Vascular tissues.

697
698
699

TOC Graphic



700
701
702